A new reliability analysis approach for the flexural capacity of postfire reinforced concrete beams retrofitted with CFRPs

Bin Cai[1,2] Bo Zhang[1] Feng Fu[2*]

1. School of Civil Engineering, Jilin Jianzhu University, Changchun, China

2.School of Mathematics, Computer Science and Engineering, City, University of London, London, UK (corresponding author: cenffu@yahoo.co.uk)

Author Photos



Bin Cai Bo Zhang Feng Fu

Abstract: This study proposed a new reliability analysis approach for the flexural capacity of postfire reinforced concrete (RC) beams retrofitted with carbon fiber reinforced polymers/plastics (CFRPs). In this approach, the thermal parameters of RC beams were determined first to enable heat transfer analysis in ABAQUS. Based on the thermal response obtained from the heat transfer analysis, a section method is used to calculate the postfire residual flexural capacity of RC beams. The reliability analysis of the beams after strength reduction was subsequently performed using the Monte Carlo method. The effects of fire exposure time, concrete cover thickness, and CFRP reinforcement ratio on the reliability of the flexural capacity of RC beams after fire exposure were studied. This new approach was found to be accurate and effective. It provided an effective reliable model for the evaluation of the mechanical properties of post-fire RC beams strengthened with CFRPs and subsequent reliability analysis.

Keywords: Concrete structures; Composite structures; Fire engineering; CFRP; Reliability; Monte Carlo method

[*] Corresponding author: E-mail address: cenffu@yahoo.co.uk

1. Introduction

Building fires have caused catastrophic damage to human lives and properties, and the effects of building fires pose tremendous safety risks. In China, building fires resulted in approximately 1582 deaths and 1065 casualties in 2016 alone. Moreover, these fires severely destroyed civil infrastructure, leading to governmental property losses worth 3.72 billion RMB (NBS,2017).

Fire mitigation involves multiple aspects, and one of the major measures is to retrofit the structural systems of buildings after fires to ensure the structures satisfy certain design requirements (Bamonte and Monte, 2015; Fei *et al*., 2017). Retrofitting post-fire reinforced concrete (RC) structures is an urgent problem that must be solved by the international industrial community.

The most commonly used material for structural retrofitting is carbon fiber reinforced polymer/plastic (CFRP), which exhibits high strength and corrosion resistance and can be rapidly constructed. The excellent properties CFRPs enable these materials to be mounted to the bottom of beams or plates to provide additional bending strength. CFRPs can also be added at the sides of beams for enhanced shear capacity, whereas CFRP retrofitted joints of columns or beam-columns could offer additional confinement and ductility (Balsamo *et al*., 2005). Thus, CFRPs are widely used to reinforce and repair RC components after fires.

1.1 Existing Research

The residual capacity of the structural components exposed to fire have been studied in the past decades. Xu (2013) tested the mechanical properties of reinforced concrete beams after fire. The calculation method of shear capacity of three-sided heated RC beams was proposed. However, the flexural capacity of RC beams after fire was not discussed in depth. Therefore, further theoretical calculation of the flexural capacity of RC beams after fire is to be carried out in this paper. Rush (2017) carried out fire exposure tests with RC columns and found that the fire intensity defined by commonly used equivalent fire duration was unable to appropriately explain the complex variation in mechanical properties of concrete columns during fire exposure. Kodur (2016) proposed a finite element method (FEM) model for evaluating the postfire residual bearing capacity of RC beams and to analyze under real engineering cases, and their results showed that this model can be used to assess the postfire bearing capacity of RC beams in practical engineering applications. Eamon (2013a;2013b) analyzed the reliability of RC columns under fire loading and proposed a prestressed concrete column reliability model under fire loading. Yao and Hu (2015) studied the performance of concrete-filled steel tubular columns after fire exposure and proposed a simplified method for evaluating the residual strength of concrete-filled steel tubular columns. Behnam (2017) proposed a CFRP reinforcement method that effectively improved the fire resistance and load carrying capacity of the building. Firmo (2012) conducted experimental and numerical studies on the post-fire mechanical properties of RC beams strengthened with CFRP and recorded the time of CFRP shedding. Williams (2008) studied the performance of FRP-strengthened RC T-beams under standard fire conditions and measured their fire resistance. Ardalani (2017) tested the bending properties of CFRP-reinforced RC beams in six different sizes and discussed the effects of beam size on mechanical properties. Siddiqui (2010) investigated the bending, shear strength and mechanical properties of CFRP-reinforced RC beams and found that U-shaped CFRP sheets effectively improved the flexural capacity of the beams, whereas inclined CFRP plates bonded to the side surfaces of RC beams significantly enhanced the shear capacity of the beams. Feng (2018) tested the CFRP-reinforced concrete circular steel columns and found that the reinforcing effect increased with increasing CFRP strength. Alsayed (2010a,2010b) studied CFRP-reinforced beam-column joints and found that CFRP significantly enhanced the flexural and shear capacities of beam-columns and delayed the rigidity deterioration.

Some research has also been performed on the reliability analysis of CFRP-strengthened structural members. Alsayed (2013) analyzed the reliability of CFRP-strengthened shear-deficient RC beams and found that the expected reliability of shear capacity could be achieved by altering the CFRP size. Bigaud (2014) analyzed the reliability of CFRP-strengthened RC bridges and found that the reliability was largely affected by the erosion of steel reinforcements and only slightly affected by the fatigue of concrete.

1.2 Research significance

The CFRP can significantly improve the flexural capacity of RC beams after fire, therefore, some of the structural elements can be reused after their exposure to the fire. However, the reliability of this retrofitting method has not been assessed in detail. Whether the retrofitted beam can have sufficient flexural capacity to be re-used in its remain life cycle is not clear.

However, from above literature review, there is insufficient research on the reliability of the flexural capacity of postfire RC components retrofitted using CFRP. Post-fire assessment of concrete quality is relevant due to the need to take a decision on the possibility of further operation of the facility after fire accident. The safety of fire-damaged beams retrofitted by CFRP is a major concern. The failure of a reinforced beam will cause substantial losses and the various factors related to failure are highly random and variable. At present, the mechanical properties of reused concrete components retrofitted using CFRP after fire conditions is not clear. Jiang (2013) studied the reliability analysis of reinforced concrete member under fire load. Yuan (2017) analyzed the reliability of shear capacity of reinforced concrete beams. Wang (2008) studied the reliability of four-face fired reinforcement concrete columns. Gong (2000) analyzed the reliability of reinforced concrete axially compressed members after rehabilitation. However, the reliability analysis of the flexural capacity of RC members retrofitted by CFRP is rarely studied. In many cases, the actual structure has different criteria for security in different states. This requires introducing a uniform indicator to describe their performance in order to assess the structural security.

In real design practice, limit state design principles are all based on reliability theory. However, in many cases, although the strength of the existing structural members is calculated according to the normative design formula, the structure is not guaranteed to be absolutely safe or reliable, because there are still uncertain factors affecting the reliability of the structure, such as the uncertainty of the properties of the reinforced concrete after fire, the uncertainty of the geometric parameters of the component, the uncertainty of the calculation model and the variability of the load. Only when the reliability of the bearing capacity of the reinforced concrete structure after fire is clarified, can the structural design be carried out. The purpose of this study is to evaluate the relationship between the safety factors of the structure design from design code and the target reliability in order to fully evaluate the structural safety of FRP retrofitted beam after fire for continued use.

Therefore, it is necessary to study and analyze the reliability of such beams and determine the key factors affecting reliability. As little research has been performed, the study is of practical and research significance It is imperative to investigate the reliability of the retrofitted beam after fire, the research presented in this paper is timely.

1.3 new reliability analysis approach

In this study, a new approach was proposed for the reliability analysis of the flexural capacity of postfire RC beams retrofitted with CFRPs. Based on this approach, the effects of fire exposure time, concrete cover thickness, and CFRP reinforcement dosage on the flexural capacity reliability of RC beams were investigated. A new process was used in this research to evaluate the reliability of the flexural capacity of postfire RC beams strengthened with CFRPs. The flow chart for this process is shown in Fig. 1.

(1) Heat transfer analysis: During fire exposure, temperature differences exist among different sectional points, which indicates that the temperature distribution of each component must be analyzed before calculating the postfire residual flexural capacity of RC beams. Therefore, standard fire temperature curves, material thermal properties and thermodynamic equations were selected to build FEM temperature analysis models corresponding to different duration of fire exposure; these models were built in the FEM software ABAQUS. The FEM temperature analysis models were used to analyze the temperature fields with respect to the fire exposure duration.

(2) Calculation of flexural capacity: The mechanical properties of both steel reinforcements and concrete deteriorated after fire exposure, which results in lower flexural capacity that subsequently caused increased safety risks. Thus, before reliability analysis, the flexural capacity attenuation of components should be quantitatively analyzed. The temperature of postfire RC beams was determined from the heat transfer analysis using ABAQUS. Strength reduction equations were introduced to determine the postfire strength of the component materials. Then, the postfire residual flexural capacity of both RC beams and CFRP-strengthened RC beams was analyzed.

(3) Reliability analysis: Based on the component residual capacity and the loading effect, probability models concerning the random variables related to the component load and the flexural capacity effect were developed. A function for the postfire flexural capacity of CFRP-reinforced RC beams was developed and programmed in MATLAB. Then, the reliability of postfire RC beams strengthened with CFRPs was calculated and the results were analyzed.

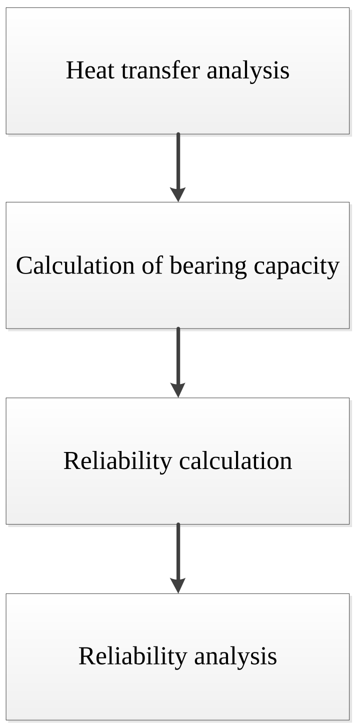

Fig. 1 Flow chart of the new reliability analysis process

2. Calculation of postfire flexural capacity

2.1 Heat transfer analysis

The component temperature was determined first. The computation of the temperature distribution was dependent on the thermal properties of the materials, and the calculation of the postfire residual flexural capacity required the postfire mechanical properties of the materials.

It is worthwhile to introduce some basic heat transfer knowledge here for a better understanding of the behavior of the structure under fire (Fu,2015).

2. 1. 1 Heat transfer analysis theory

a. **Conduction**

Conduction is the mechanism in solid materials, in the steady-state situation, the transfer of heat by conduction can be calculated as follows:

$$q = kdT / dx \tag{1}$$

where q is the heat flow per unit (W/ m^2), k is the thermal conductivity, T is the temperature, and x is the distance in the direction of heat flow.

b. **Convection**

Convection is the heat transfer by the movement of fluids, either gases or liquids, convective heat transfer is an important factor in flame spread and the transport of smoke and hot gases. It can be calculated as follows:

$$q = h\Delta T_s \tag{2}$$

where h is the convective heat transfer coefficient (W/ m^2K), ΔT_s is the temperature difference between the surface of the solid and the fluid.

c. **Radiation**

Radiation is the transfer of the energy by electromagnetic waves. It is extremely important in fire as it is the main mechanism for heat transfer. It can be decided as follows:

$$q = \varphi\varepsilon\sigma(T_e^4 - T_r^4) \tag{3}$$

where φ is the configuration factor, ε is Stefan-Boltzmann constant (5.67x10^{-8}W/m^{2}K^4), T_e is the absolute temperature of emitting surface (K)., and T_r is the absolute temperature of receiving surface (K).

d. **Specific Heat**

The specific heat is the amount of heat per unit mass required to raise the temperature by one degree Celsius. The relationship between heat and temperature change is usually expressed in the form shown below. The relationship does not apply if a phase change is encountered, because the heat added or removed during a phase change does not change the temperature.

$$Q = cm\Delta T \tag{4}$$

where Q is the heat added, c is the specific heat, m is the mass, and ΔT is the change in temperature.

2.1.2 Thermal properties of the materials

The thermal properties of the materials included heat conductivity, specific heat, which were the basis for computing the temperature distributions. Since the thermal models in BS EN1994-1-2 (BSI, 2013) performed well in computing the temperature fields of RC beams, the thermal properties from BS EN1994-1-2 (BSI, 2013) were used here in (Eqs. (5) - (8)):

The specific heat capacity of concrete, c_c:

$$c_c = 900 - 4\left(\frac{T}{120}\right)^2 + 80\left(\frac{T}{120}\right) \quad 20°C \le T \le 1200°C \tag{5}$$

where T is the current temperature.

The heat conduction rate of concrete, λ_c:

$$\lambda_c = 2 - 0.24\left(\frac{T}{120}\right) + 0.012\left(\frac{T}{120}\right)^2 \quad 20°C \le T \le 1200°C \tag{6}$$

The specific heat capacity of steel, c_s:

$$c_s = \begin{cases} 425 + 7.73\times10^{-1}T - 1.69\times10^{-3}T^2 + 2.22\times10^{-6}T^3 & 20°C \le T < 600°C \\ 666 + \dfrac{1302}{738 - T} & 600°C \le T < 735°C \\ 545 + \dfrac{17820}{T - 731} & 735°C \le T < 900°C \\ 650 & 900°C \le T < 1200°C \end{cases} \tag{7}$$

The heat conduction rate of steel, λ_s:

$$\lambda_s = \begin{cases} 54 - 3.33\times10^{-2}T & 20°C \le T \le 800°C \\ 27.3 & 800°C < T \le 1200°C \end{cases} \tag{8}$$

The ISO-834 fire curve was adopted in this study, which can be expressed as follows (ISO,1999):

$$T = T_0 + 345\lg(8t + 1) \tag{9}$$

where T_0 is the room temperature and t is the heating time.

2.1.3 Heat Transferring analysis

After fire exposure, the mechanical properties of the material are mainly related to the maximum temperature experienced by the member. The maximum temperature of each point in a component can determine the maximum temperature field during fire exposure. The mechanical properties of the components after fire exposure are mainly related to the maximum temperature attained during the fire. The maximum temperature for different time duration were simulated using the FEM software ABAQUS. The thermal parameters of the materials were determined according to Eqs. (5) - (8). As only maximum fire temperature is needed, therefore ISO-834 fire curve was used to simulate the room temperature rather than the parametric fire temperature.

The concrete was modeled with DC3D8 eight-node linear heat transfer hexahedron units, whereas the steel reinforcement was modeled with DC1D2 two-node heat transfer connected units. The temperature distribution of these two materials were both simulated according to ISO-834 fire curve.

2.2 Method to calculate postfire flexural capacity

The mechanical properties of the components were deteriorated after fire exposure. Therefore, the temperature distributions of components determined from the temperature fields can be used to calculate the postfire flexural capacity of the beam.

2.2.1 Strength degradation of materials

The compressive strength reduction factor of postfire concrete was calculated as follows (Wang and He, 2009):

$$\varphi_{CT}=\frac{f_{\mathrm{cr}}(T)}{f_{\mathrm{c}}}=\begin{cases}1.0 & 0°C<T\le 200°C\\ \left[1.0-0.0015(T-200)\right] & 200°C<T\le 500°C\\ \left[0.25+0.003(600-T)\right] & 500°C<T\le 600°C\\ \left[0.25-7.5\times10^{-4}(T-600)\right] & 600°C<T\le 800°C\end{cases} \tag{10}$$

where $f_{\mathrm{cr}}(T)$ is the compressive strength of postfire concrete at T °C, f_{c} is the compressive strength of concrete at normal temperature, and φ_{CT} is the compressive strength reduction factor of postfire concrete.

The yield strength reduction factor of postfire steel reinforcement was computed as follows (Shen *et al.*, 1991):

$$\varphi_{yT}=\frac{f_{\mathrm{yr}}(T)}{f_{\mathrm{y}}}=\begin{cases}(99.838-0.0156T)\times10^{-2} & 0°C<T<600°C\\ (137.35-0.0754T)\times10^{-2} & 600°C\le T\le 900°C\end{cases} \tag{11}$$

where $f_{\mathrm{yr}}(T)$ is the yield strength of postfire steel reinforcement at T °C, f_{y} is the yield strength of steel reinforcement at normal temperature, and φ_{yT} is the yield strength reduction factor of postfire reinforced steel at T °C.

2.2.2 Calculation of postfire flexural capacity

After the temperature distributions and postfire material strength reduction factor was determined using the section method of several existing literatures (EI-Fitiany and Youssef, 2017). In this method, the beam section is divided into equal height small rectangular cross section, and correspondent stress blocks can be obtained. As it shown in Fig. 2, the height x of the compressive zone in postfire component can be computed based on and Eq. (12):

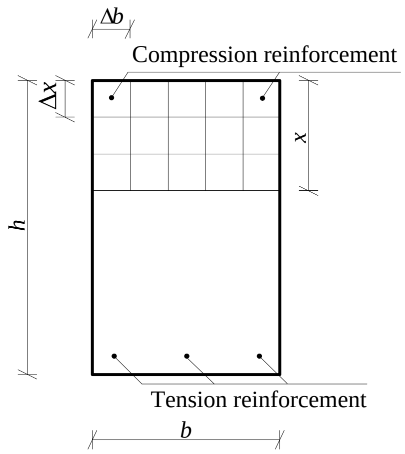

Fig. 2 Element division of compressive zone of postfire beams

$$f_c \sum \bar{\varphi}_{CT_i} \Delta b \Delta x + \varphi'_{yT} f'_y A'_s = \varphi_{yT} f_y A_s \tag{12}$$

where $\bar{\varphi}_{CT_i}$ is the compressive strength reduction factor of the concrete in zone i, which is calculated by substituting the highest temperature T_i in zone i into Eq. (10); φ'_{yT} is the yield strength reduction factor of compressive steel reinforcement; and f'_y is the yield strength of compressive steel reinforcement at normal temperature.

The strength reduction factor of concrete in the compressive zone was calculated as follows:

$$\bar{\varphi}_{CT} = \frac{\sum \bar{\varphi}_{CT_i} f_c \Delta b \Delta x}{f_c b x} \tag{13}$$

where x is the height of the compressive zone in the postfire component.

The flexural capacity of postfire concrete beams was calculated as follows:

$$M_{CT} = \alpha_1 \bar{\varphi}_{CT} f_c b x \left(h_0 - 0.5x\right) + \varphi'_{yT} f'_y A'_s \left(h_0 - a'_s\right) \tag{14}$$

where M_{CT} is the flexural capacity of postfire concrete beams with maximum fire temperature of T ºC, b is the sectional width of beams, h_0 is the valid sectional height of beams, $\alpha_1 = 1$, A'_s is the area of steel reinforcement in the compressive zone, and a'_s is the distance from the resultant force point of the compressive steel reinforcement to the margins of the compressive section.

Above calculation based on below basic assumptions are used in the calculation:

1. The concrete strength after fire in each small rectangular cross section is constant;

2. The equivalent concrete strength reduction coefficient of the whole compression zone can be obtained by weighted average on the area of the compression zone.

3. Ignore the contribution of the concrete in the tension zone.

2.3 Validation

2.3.1 *Temperature distribution validation*

The FEM models built in Section 3.1 were used to simulate the temperature fields at 5 temperature measuring points on beams with 3 surfaces exposed to fire, and the results are shown in Fig. 3. The calculated results were compared with the testing data for high-temperature RC beams reported in Ref. (Xu *et al.*,2013).

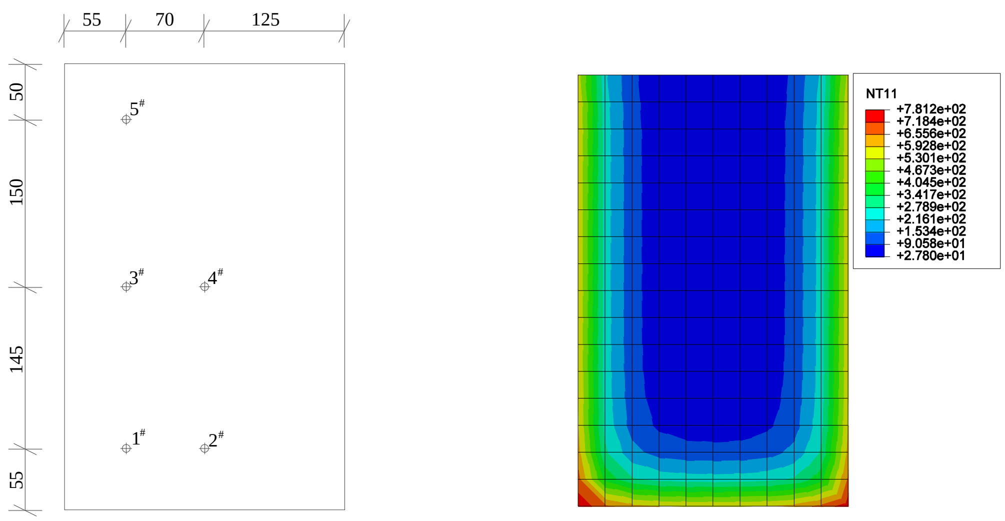

(a) Temperature measuring point (b) Fire exposure for 30 min

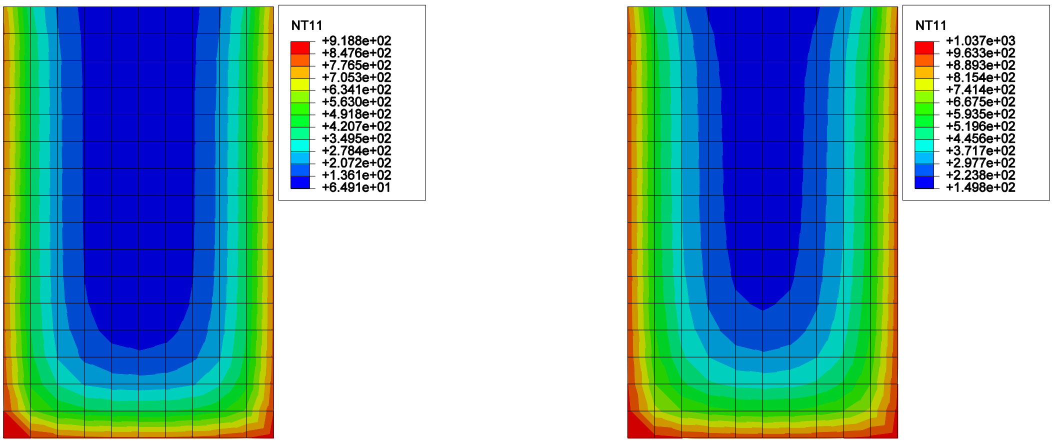

(c) Fire exposure for 60 min (d) Fire exposure for 120 min

Fig. 3 Temperature distributions at beam sections

Since the fire-exposed surfaces were in direct contact with the air, the hot air transferred heat via heat convection and radiation to the fire-exposed surfaces. Thus, the temperatures in the beams were the highest at the exposed surfaces, and the temperature in these points increased more rapidly than the other measure points; the temperature at the nonexposed surface was the lowest.

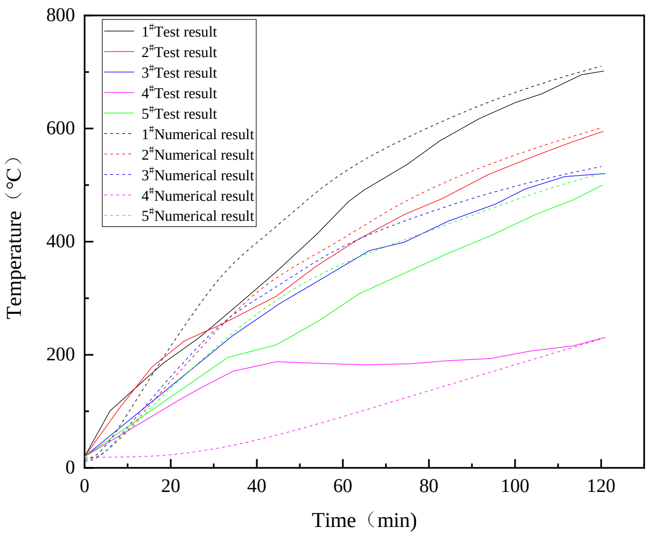

Fig. 4 Temperature-time curve contrast with XU's experiments

The experimental temperature-time relations and the FEM-simulated temperature-time relations are shown in Fig. 4. Clearly, the calculated results based on the FEM software were generally consistent with the experimental results obtained by Xu et al. (2013), but there were some deviations because the temperature of the components increased quickly after the outer concrete peeled off or burst during fire exposure.

2.3.2 Validation of the postfire flexural capacity

The experimental results from Ref. (Xu *et al*.,2013) were used to validate the postfire residual flexural capacity. The specimen L5 was the test beam for testing the flexural capacity after fire, and L5 in the literature was used to verify the residual capacity after fire. Based on the sectional temperature distributions in Fig. 3 and the postfire flexural capacity model in Section 2.2, the postfire residual flexural capacity of specimen L5 was calculated to be 202.6 kN·m. The error of the result was 3.3% from the value of 196 kN·m reported in Ref. (Xu *et al*.,2013), indicating that the postfire flexural capacity was consistent with the results from Ref. (Xu *et al*.,2013); hence, this method can be used in reliability computation.

3. Reliability analysis

3.1 RC beam design

For normal design conditions, the structural response should satisfy:

$$M_{\mathrm{sd}} \le M_{\mathrm{rd}} \tag{15}$$

where M_{sd} is the design value of the bending moment induced by the design loads and M_{rd} is the design value of the bending moment capacity.

When calculating the design value of the bending moment induced by the load, the most unfavorite design value should be used (GB,2012):

$$M_{\mathrm{sd}} = \max\left\{\left(\xi\gamma_{\mathrm{G}}M_{\mathrm{G}} + \gamma_{\mathrm{Q}}M_{\mathrm{Q}}\right);\left(\gamma_{\mathrm{G}}M_{\mathrm{G}} + \gamma_{\mathrm{Q}}\psi_{\mathrm{c}}M_{\mathrm{Q}}\right)\right\} \tag{16}$$

where ξ is a reduction factor for unfavorable permanent loads, γ_G is the partial factor for the permanent load, M_G is the bending moment induced by the characteristic value of the permanent load, M_Q is the bending moment induced by the characteristic value of the variable load, γ_Q is the partial factor for the variable load, and ψ_c is a combination factor.

3.2 Determination of limit state function

During structure reliability analysis, the limit state function can be written as:

$$Z = R - S = g\left(X_1, X_2, \ldots X_n\right) \tag{17}$$

where $g(X)$ is the failure function, X_1, X_2, …X_n are n mutually independent random variables, R is the resistance of the structure, and S is the action effect of the structure. Values of Z greater than 0, less than 0, or equal to 0 indicate that the structure is under a reliable status, a failure status or a limit status, respectively.

The flexural capacity of RC beams at normal temperature was (GB,2010):

$$M_C = \alpha_1 f_c bx\left(h_0 - 0.5x\right) + f_y' A_s'\left(h_0 - a_s'\right) \tag{18}$$

where M_C is the flexural capacity of RC beams at normal temperature.

During the calculation of flexural capacity, the basic assumptions did not fully agree with reality, and approximations of the calculated results led to variation in the bearing capacity. Therefore, we introduced a random variable γ_m that represents the uncertainty coefficient of the resistance calculation, which can be used to describe the variability in the calculated results of bearing capacity. The limit state function of RC beams at normal temperature is:

$$Z = R - S = \gamma_m M_C - \left(M_{Gm} + M_{Qm}\right) \tag{19}$$

where M_{Gm} is the mean value of M_G and M_{Qm} is the mean of M_Q.

The limit state function of postfire RC beams is:

$$Z = R - S = \gamma_m M_{CT} - \left(M_{Gm} + M_{Qm}\right) \tag{20}$$

Since the flexural capacity of RC beams was deteriorated after fire exposure, CFRPs can be used to reinforce the bottom of postfire RC beams. If the bonding between CFRP and concrete is assumed to be perfect (GB,2013), the flexural capacity of postfire CFRP-reinforced RC beams can be computed as follows:

$$M_{\mathrm{D}} = \alpha_1 \bar{\varphi}_{\mathrm{C}T} f_{\mathrm{c}} bx\left(h-0.5x\right)+\varphi'_{\mathrm{y}T} f'_{\mathrm{y}} A'_{\mathrm{s}}\left(h-a'_{\mathrm{s}}\right)-\varphi_{\mathrm{y}T} f_{\mathrm{y}} A_{\mathrm{s}}\left(h-h_0\right) \tag{21}$$

$$x=\left(\varphi_{\mathrm{y}T} f_{\mathrm{y}} A_{\mathrm{s}} + \psi_{\mathrm{f}} f_{\mathrm{fu,s}} A_{\mathrm{fe}} - \varphi'_{\mathrm{y}T} f'_{\mathrm{y}} A'_{\mathrm{s}}\right) / \left(\alpha_1 \bar{\varphi}_{\mathrm{C}T} f_{\mathrm{c}}\right) \tag{22}$$

where M_{D} is the flexural capacity of postfire RC beams strengthened with CFRPs, $f_{\mathrm{fu,s}}$ is the mean tensile strength of CFRPs, A_{fe} is the valid sectional area of CFRPs, and ψ_{f} is the strength use coefficient of CFRPs.

The limit state function of postfire RC beams strengthened with CFRPs was determined from Eq. (23):

$$Z = R - S = \gamma_{\mathrm{m}} M_{\mathrm{D}} - \left(M_{\mathrm{Gm}} + M_{\mathrm{Qm}}\right) \tag{23}$$

3.3 Statistical parameters of the variables

When the Monte Carlo method is used to calculate the structural reliability, a probability model with correspondent random variables should be used. The random variables used in this study are determined from large-scale data analysis and tests. The concrete parameters are listed in Table 1. As shown in Table 1, these statistical parameters are selected based on the Chinese Code (GB2010), BS(2004) and the research of Cai(2016) and (Coile et al.,2014).

Table 1 Probabilistic models for the basic variables of the analyzed concrete beams

Symbol	Variable	Distribution	Units	Bias[a](mean)	CoV[b](std[c])	Nominal value	Source
f_c	C30 compressive strength	Log-normal	MPa	1.395	0.15	20.1	(GB,2010)
f_y	HRB335 steel yield stress	Log-normal	MPa	1.139	0.07	335	(GB,2010)
S_Q	Live load	Extreme type I	kN·m	0.859	0.233	-	(GB,2012)

$\boldsymbol{S}_{\mathbf{G}}$	Dead load	Normal	kN·m	1.060	0.070	-	(GB,2012)
$\boldsymbol{h}_{\mathbf{0}}$	Effective depth of section	Normal	mm	1.000	0.030	565	(CAI *et al.*,2016)
$\boldsymbol{b}$	Beam width	Normal	mm	1.000	0.010	250	(CAI *et al.*,2016)
$\boldsymbol{A}_{\mathbf{f}}$	CFRP cross-sectional area	Normal	mm^2	1.00	0.02	-	(CAI *et al.*,2016)
$\boldsymbol{f}_{\mathbf{f}}$	CFRP tensile strength	Weibull	MPa	1.152	0.08	3100	(CAI *et al.*,2016)
$\boldsymbol{\gamma}_{\mathbf{m}}$	Total model uncertainty	Normal	-	1	0.025	-	(Coile *et al.*,2014)
$\boldsymbol{t}_{\mathbf{f}}$	CFRP strip thickness	Log-normal	mm	1.00	0.010	0.167	(CAI *et al.*,2016)
$\bar{\varphi}_{CT}$	*T* (°C) concrete compressive strength reduction factor	Beta	-	(Temperature dependent, conforms to EN 1992-1-2)	(Temperature dependent)	-	(BSI, 2004)
$\varphi_{yT}\left(\varphi'_{yT}\right)$	*T* (°C) reinforcement yield stress reduction factor	Beta	-	(Temperature dependent, conforms to EN 1992-1-2)	(Temperature dependent)	-	(BSI, 2004)

[a]Bias:mean value/nominal value

[b]CoV:coefficient of variation

[C]std:standard deviation

To measure the errors of the analysis caused by different loading values, the following load ratio was introduced:

$$n = M_{\mathrm{Qm}} / M_{\mathrm{Gm}} \tag{24}$$

where the sum of $M_{\mathrm{Qm}} + M_{\mathrm{Gm}}$ is constant; n is typically in the range of 0.1 - 2.

3.4 Reliability calculation based on the Monte Carlo simulation method

The Monte Carlo method, also called a random sampling method, essentially aims to simulate numerous statistical data according to the probability distribution of the data. Each simulation represents a completed mechanical analysis of the component. Through the number of failures and non-failures of the obtained components, the reliability is obtained statistically, and its simulated precision is directly affected by the size of simulated sample. In the Monte Carlo simulation method, the limit state function and the probability model of random variables were used in 10^6 repeated simulations in Matlab, and the reliability was accurately calculated. The specific procedures are listed as follows (Fig. 5):

(1) A mechanical property reduction model, which calculated the flexural capacity of postfire RC beams strengthened with CFRPs and postfire RC beams, was built;

(2) A failure function $g(X)$ was built based on this mechanical model;

(3) The random variables of the limit state function were integrated with their probability distributions;

(4) Random values were simulated repeatedly using the Monte Carlo method with the probability distribution of random variables, and $g(X)$ was calculated using the simulated values;

(5) When the number of repetitions reached the preset value, the simulations were terminated, and the reliability was computed using $g(X)$.

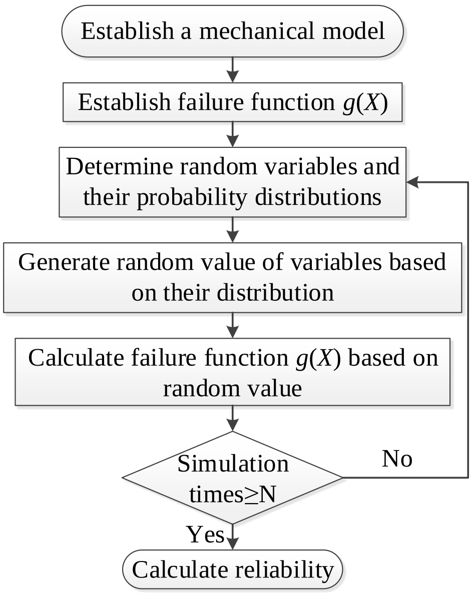

Fig. 5 Flow chart for reliability analysis based on the Monte Carlo method

4. Case study

A case study is performed here to illustrate the process of the reliability analysis method proposed in this paper.

4.1 Numerical simulation of the temperature distribution in the beam

RC beams with sectional sizes of 250×600 mm^2 were selected, and these beams were composed of C30 concrete. Then, the loads were determined, and the elements were reinforced. The compressive and tensile reinforcement was HRB335 steel rebar. Three tensile steel rebars with diameters of 32 mm and two compressive steel rebars with diameter of 22 mm were used. The HRB335 stirrup was 10 mm in diameter, and the stirrup spacing was 150 mm. The elements were analyzed under two conditions, which were divided by the concrete cover thickness. First, the concrete cover thickness was set to 19 mm, which corresponds to a value of 35 mm (a_s is the distance from the resultant force point of the tensile steel to the margins on the concrete section) for the sum of the concrete cover thickness and the longitudinal steel radius. Second, the concrete cover thickness was set to 29 mm, which similarly corresponds to a value of 45 mm. The lower part of a structure, or the bottom and two lateral faces of the beam, was exposed to fire to replicate a realistic fire scenario. Since the bearing capacity was weakened after fire exposure, different numbers of CFRP layers (200 mm wide and 0.167 mm thick, with a tensile strength of 3100 Mpa) were used to reinforce the bottom of the elements.

The fire exposure status of each RC beam was simulated with the FEM software ABAQUS. Assume that there is good heat transfer between the steel and the concrete, there is no thermal resistance, so the bonded contact method is adopted. The concrete was modeled with DC3D8 elements, and the mesh size was 0.03 m. The longitudinal steel and stirrup were modeled with DC1D2 elements, the mesh size for the longitudinal steel was 0.53 m, and the mesh size for the stirrup was 0.053 m. The same meshing method was used in the two situations. To simulate the temperature fields, the RC beams were exposed to fire for 30, 60 or 120 min based on the ISO-834 fire curve, which replicates real fire exposure conditions. The temperature distributions of the concrete are as follows (Fig. 6).

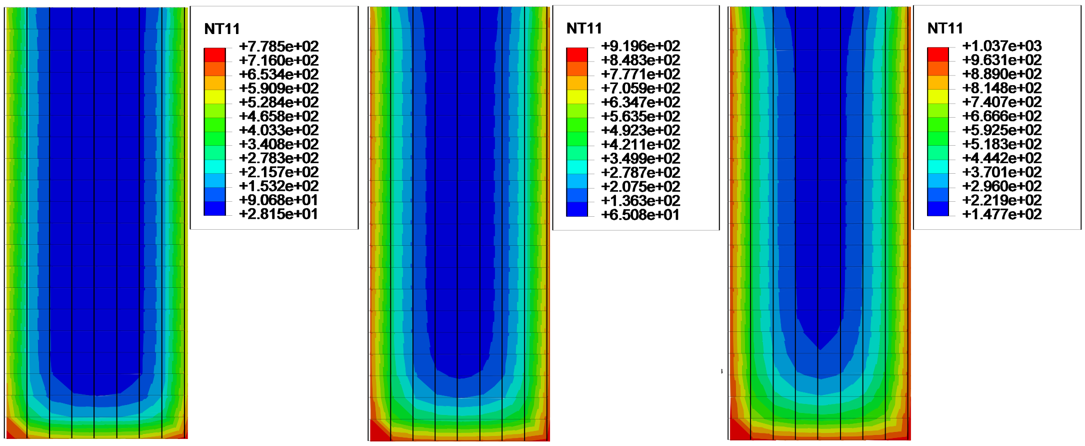

(a) Fire exposure for 30 min (b) Fire exposure for 60min (c) Fire exposure for 120min

Fig. 6 Temperature distributions at beam sections (ºC)

The steel temperature distribution is a prerequisite for calculating the steel yield strength reduction factor. Steel temperatures were determined by summarizing the steel temperature distributions (Table 2).

Table 2 Steel temperature distributions

Working	Steel	Temperatures of	Temperature of the

conditions	temperature at upper part (ºC)	two external steel bars at lower part (ºC)	middle steel bar at lower part (ºC)
a_s=35 mm, FE=30 min	190	315	205
a_s=35 mm, FE=60 min	355	544	382
a_s=35 mm, FE=120 min	534	817	612
a_s=45 mm, FE=30 min	150	240	162
a_s=45 mm, FE=60 min	292	464	320
a_s=45 mm, FE=120 min	470	715	550

Note: FE = fire exposure

Clearly, due to the thermal inertia of concrete, the temperature distributions of postfire elements are U-shaped, and the temperatures gradually diffused from the outer surfaces of the concrete to the interior of the concrete as the fire exposure time increased (Fig. 6). The steel temperature also gradually increased as the fire exposure time increased. The steel temperature within the same fire exposure time decreased with the increasing concrete cover thickness. Increases in the concrete cover thickness delayed the temperature increase in the steel to some extent (Table 2). The temperature distribution directly shows the trend and variation in the temperature transfer inside the elements.

4.2 Reliability analysis

In this case, the reliability analysis process accounted for the effects of different load ratios, fire exposure time and CFRP dosages after fire exposure on the flexural capacity reliability.

(1) Reliability of RC beams at normal temperature

M_G and M_Q were determined from Eq. (16), and we subsequently determined that M_{sd}=364.7 kN·m, A_s =2413 mm, and A_s' =760 mm. With the data in Table 1, the value of M_{sd} was converted to M_{Qm}+M_{Gm}=282 kN·m. Then, different load ratios n and a_s conditions were selected. Eq. (24) was then used to determine the values of M_{Qm} and M_{Gm} with different values of n. Programs combining Eq. (19) with the Monte Carlo method were conducted in MATLAB. The reliability index β was calculated for the elements at normal temperature and with different values n values.

(2) Reliability of RC beams after fire exposure

The flexural capacity of RC beams after different durations of fire exposure were calculated via Eq. (16). The Monte Carlo method program established in MATLAB was conducted to determine the reliability index β of the flexural capacity of the elements exposed to fire under different fire exposure time and different load ratios n and a_s conditions. In the calculation process, the load was assumed to be constant.

(3) Reliability of reinforced RC beams after fire exposure

After different duration of fire exposure, RC beams were reinforced with CFRPs. The CFRP dosage conditions were calculated with Eq. (19) and the Monte Carlo method program established in MATLAB was conducted to determine the reliability index β of the elements exposed to fire under different fire exposure time, CFRP dosages, load ratios n and a_s conditions. In the calculation process, the load was assumed to be constant.

4.3 Results and discussion

In the reliability analysis process, the effects of the load ratio, CFRP dosage, concrete cover thickness and temperature on the reliability index were studied to understand the reliability of postfire RC beams retrofitted with CFRPs. To study the effects of the load ratio, fire exposure time, concrete cover thickness, and CFRP dosage on the reliability index of flexural capacity of RC beams, we selected concrete cover thickness a_s=35 and 45 mm, fire exposure time for 0, 30, 60 and 120 min, load ratios n of 0.10, 0.25, 0.50, 0.75 and 1.00, and CFRP disages of 0 layer (0 mm), 1 layer (0.164 mm), 2 layers (0.328 mm) and 3 layers (0.492 mm).

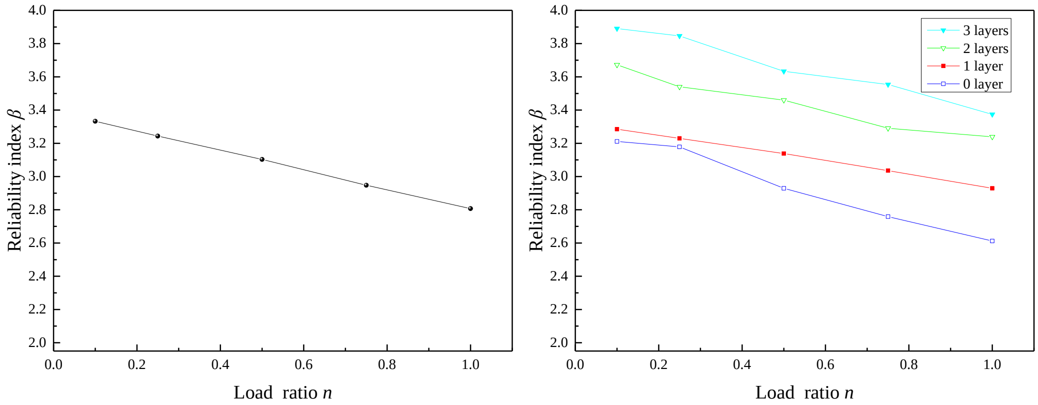

(a) Fire exposure for 0 min (b) Fire exposure for 30 min

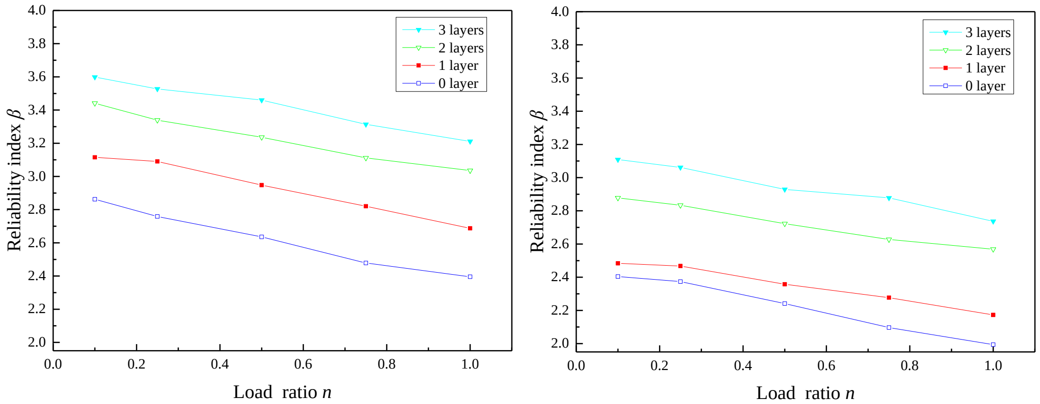

(c) Fire exposure for 60 min (d) Fire exposure for 120 min

Fig. 7 Effects of different factors on the reliability index when a_s =35 mm

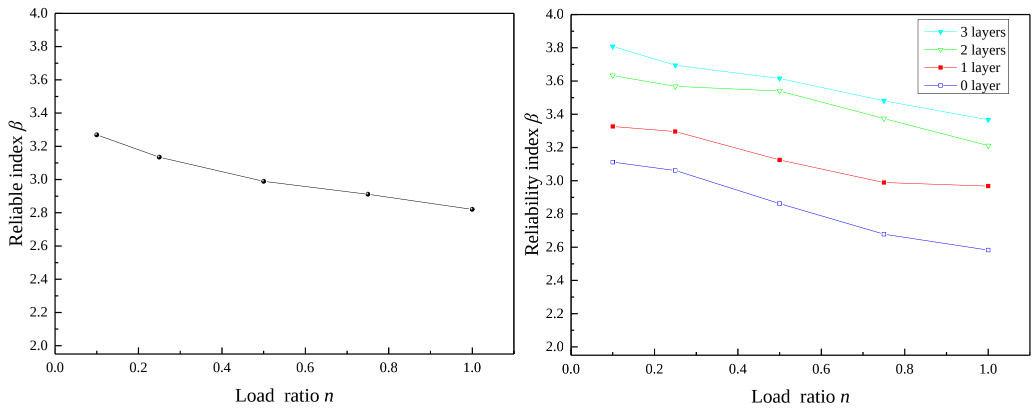

(a) Fire exposure for 0 min (b) Fire exposure for 30 min

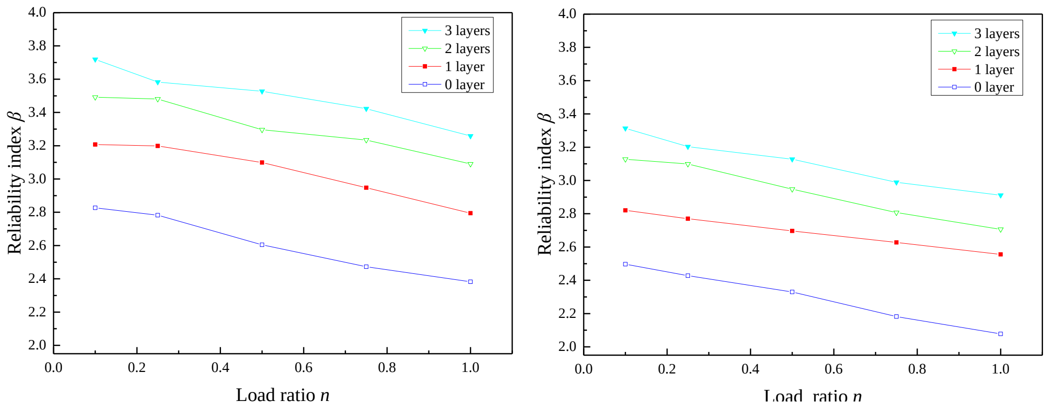

(c) Fire exposure for 60 min (d) Fire exposure for 120 min

Fig. 8 Effects of different factors on the reliability index when a_s = 45 mm

A reliability analysis process is proposed for postfire RC beams strengthened with CFRPs (Figs. 7 and 8). RC beams strengthened by 2 layers (0.328 mm) after 30 or 60 min of fire exposure can meet the specification (GB, 2001): the reliability index of the second-class ductile component should be greater than 3.2, but after 120 min of fire exposure, the reliability of the beams did not satisfy the specification (GB, 2001) even when 3 layers (0.492 mm) were used. At the same load ratio, as the fire exposure time increased, the reliability index of the component at a_s=45 mm was larger than that at a_s=35 mm (Figs. 7c, 7d, 8c and 8d). This finding occurred because the increase in concrete cover thickness slowed the temperature increase in the steel reinforcement to some extent, indicating that the strength of the steel reinforcement at a_s=45 mm was slightly greater than that at a_s=35mm. At the same load ratio, as the fire exposure time increased, the reliability index of the components gradually decreased, especially at a_s=35 mm (Figs. 7 and 8). At the same load ratio, as the CFRP thickness increased, the reliability index of the components increased (Figs. 7b-d and 8b-d).

The increasing efficiency of postfire flexural capacity in the CFRP-strengthened RC beams was computed at a load ratio of 0.2.

Table 3 Efficiency of the postfire reliability index

(a) Efficiency of the postfire reliability index of the CFRP-strengthened RC beams when a_s=35 mm.

Fire exposure time	1 layer of CFRP	2 layers of CFRP	3 layers of CFRP
30 min	2.28%	14.34%	21.14%
60 min	8.81%	20.19%	25.70%
120 min	3.30%	19.70%	29.28%

(b) Efficiency of the postfire reliability index of the CFRP-strengthened RC beams when a_s=45 mm

Fire exposure time	1 layer of CFRP	2 layers of CFRP	3 layers of CFRP
30 min	6.89%	16.75%	22.38%
60 min	13.45%	23.51%	31.55%
120 min	12.93%	25.26%	32.7%

At the same load ratio, at a_s=35 mm, the reliability index of RC beams strengthened by one layer of CFRP sheet did not obvious increase, but the reliability index increased significantly with two layers of CFRP (Table 3a). At a_s=45 mm, the reliability index of the RC beams increased effectively even with one layer of CFRP (Table 3b), because the increase in the concrete cover thickness slowed the temperature increase in the steel reinforcement, thereby, delaying the reduction in the steel strength to some extent.

5. Conclusions

A reliability analysis process for the flexural capacity of postfire RC beams was proposed, which consists of finite element simulations in ABAQUS, theoretical analyses, and numerical simulations in MATLAB. The reliability analysis accounted for the effects of different load ratios, a_s values, fire exposure time and CFRP dosage after fire exposure.

(1) The calculated results from this process were consistent with the testing data in a reference; thus, this process is qualified for practical engineering application. The reliability model could accurately and effectively evaluate the mechanical performance of postfire RC beams strengthened with CFRPs.

(2) The flexural capacity reliability index of RC beams decreased with increasing

load ratio or fire exposure time but increased with increasing concrete cover thickness or CFRP dosage.

(3) The reliability index of RC beams significantly increased with increasing CFRP reinforcement thickness. The addition of two 200 mm wide and 0.164 mm thick CFRP layers could significantly enhance the flexural capacity reliability index of RC beams.

(4) The reliability index of RC beams decreased after fire exposure but increased after reinforcement with CFRPs; the reinforcement enabled the repaired beams to meet some reported standards.

(5) When the structural requirements of RC beams were met, appropriately increasing the concrete cover thickness of the RC beams could slow the reduction in the postfire reliability of RC beams.

(6) This process can be used to calculate other postfire bearing capacity reliability of RC beams by simply adjusting the bearing capacity computation methods. Our research group will further use this process to calculate the postfire shear capacity reliability of RC beams.

Conflicts of interest

The authors declare that they have no conflicts of interest.

Funding statement

This work was supported by the National Key R&D Program of China (2017YFC0806100), the National Natural Science Foundation of China (nos. 51378238, 51678274), the Science and Technological Planning Project of the Ministry of Housing and Urban-Rural Development of the People’s Republic of China (no. 2017-K9-047) and the Foundation of China Scholarship Council (no.201805975002).

Data availability statement

The data used to support the findings of this study are available from the corresponding author upon request.

References

Abadel AA. (2011). Textile-reinforced mortar versus FRP as strengthening material for seismically deficient RC beam-column joints. *Journal of Composites for Construction,* **15(6)**, 920-933.

Alsayed SH, Almusallam TH, Al-Salloum YA, Siddiqui NA. (2010a). Seismic rehabilitation of corner RC beam-column joints using cfrp composites. *Journal of Composites for Construction,* **14(6)**, 681-692.

Alsayed SH, Al-Salloum, YA, Almusallam TH, Siddiqui NA. (2010b). Seismic response of FRP-upgraded exterior RC beam-column joints. *Journal of Composites for Construction,* **14(2)**, 195-208.

Alsayed SH, Siddiqui NA. (2013). Reliability of shear-deficient RC beams strengthened with CFRP-strips. *Construction & Building Materials,* **42(42)**, 238-247.

Ardalani GT, Showkati H, Teymourlouei HE, Firouzsalari SE. (2017). The performance of plate girders reinforced with CFRP plates of various lengths. *Thin-Walled Structures,* **120**, 105-115.

Balsamo A, Colombo A, Manfredi G, Negro P, Prota A. (2005). Seismic behavior of a full-scale RC frame repaired using cfrp laminates. *Engineering Structures,* **27 (5)**, 769-780.

Bamonte P, Monte FL. (2015). Reinforced concrete columns exposed to standard fire: comparison among different constitutive models for concrete at high temperature. *Fire Safety Journal,* **71(71)**, 310-323.

Behnam B. (2017).On the interaction between span length and opening ratio of RC frames under natural fires. *Proceedings of the Institution of Civil Engineers - Structures and Buildings,* **170**, 1-15.

Bigaud, D., Ali, O. (2014). Time-variant flexural reliability of RC beams with externally bonded CFRP under combined fatigue-corrosion actions. *Reliability Engineering & System Safety,* **131(3)**, 257-270.

BSI (2004) BS EN 1992-1-2:2004, Eurocode 2-Design of concrete structures-Part 1–2: General rules-Structural fire design. Structural Fire Design. BSI, London, UK.

BSI (2013) BS ENV 1994-1-2, Eurocode 4 - Design of Composite Steel and Concrete Structures - Part 1-2: General Rules; Structural Fire Design. BSI, London, UK.

CAI B, Zhao L L , Yuan Y H. (2016). Reliability of bending capacity for corroded reinforced concrete beam strengthened with CFRP. *Concrete*, **(10)**, 148-151.

Coile RV, Caspeele R, Taerwe L. (2014). Reliability-based evaluation of the inherent safety presumptions in common fire safety design. *Engineering Structures,* **77**, 181-192.

Eamon CD, Jensen E. (2013a). Reliability analysis of reinforced concrete columns exposed to fire. *Fire Safety Journal,* **62**, 221-229.

Eamon CD, Jensen E. (2013b). Reliability analysis of reinforced concrete beams exposed to fire. *Journal of Structural Engineering,* **139(2)**, 212-220.

El-Fitiany SF, Youssef MA. (2017). Fire performance of reinforced concrete frames using sectional analysis. Engineering Structures, 142, 165-181.

Feng R, Chen Y, Wei J, Huang J, Huang J, He K. (2018). Experimental and numerical investigations on flexural behaviour of CFRP reinforced concrete-filled stainless steel CHS tubes. *Engineering Structure*, **156**, 305-321.

Fei G, Hong Z, Liang H. (2017). Post -fire residual strength of steel tubular T-joint with concrete-filled chord. *Journal of Building Structures,* **139**, 327-338.

Firmo JP, Correia JR, França P.(2012). Fire behaviour of reinforced concrete beams strengthened with CFRP laminates: Protection systems with insulation of the anchorage zones. *Composites Part B: Engineering,***43**, 1545-1556.

Fu F. (2015). Advanced Modeling Techniques in Structural Design. ISBN 978-1-118-82543-3. Wiley.

GB(2001) GB 50068-2001:Unified standard for reliability design of building structures.GB，China，Beijing.

GB(2010) GB 50010-2010:Code for design of concrete structures.GB，China，Beijing.

GB(2012) GB 50009-2012:Load code for the design of building structures.GB，China，Beijing.

GB(2013) GB 50367-2013:Code for design of strengthening concrete structure.GB，China，Beijing.

ISO (International Organisation for Standardisation) (1999) ISO 834-1:Fire resistance tests – elements of building construction. Part 1:general requirements. ISO, Geneva, Switzerland.

Jiang F G, Zhao J L.(2013) Reliability analysis of reinforced concrete member under fire load. *Journal of Jilin University (Engineering and Technology Edition)*, **43(6)**:1500-1503.

Kodur, V. K. R., Agrawal, A. (2016). An approach for evaluating residual capacity of reinforced concrete beams exposed to fire. *Engineering Structures,* **110**, 293-306.

NBS. (People's Republic of China National Bureau of Statistics)(2017). China Statistical Yearbook. China，Beijing.

Rush, D., Lange, D. (2017). Towards a fragility assessment of a concrete column exposed to a real fire – Tisova Fire Test.*Engineering Structures,***150**, 537-549.

Shen R，Feng L Y，Rong K.(1991). Evaluation of rebar mechanical properties after high temperature (Fire Exposure). *Sichuan Building Science*,**(02)**,5-9.

Siddiqui NA. (2010). Experimental investigation of RC beams strengthened with externally bonded FRP composites. *Latin American Journal of Solids & Structures,* **6(4)**, 343-362.

Xu Y Y, WU B, Wang R H, Jiang M, Luo Y. (2013). Experimental study on residual performance of reinforced concrete beams after fire. *Journal of Building Structures,* **34 (8)**, 20-29.

Wang Z Q, Bai L L, Qiao M, Lv H Q. (2008). Reliability of four-face fired reinforcement concrete columns. *Huazhong University of Sci.&Tech.(Natural Science Edition)*, **36(12)**:125-127.

Wang Z Q, He J.(2009). Nonlinear analysis of reinforced concrete structures. China，Harbin.

Williams B, Kodur V, Green MF, Bisby L. (2008). Fire endurance of fiber-reinforced polymer strengthened concrete T-beams. *ACI structural journal,* **105**, 60-67.

Yao Y and Hu X X. (2015). Cooling behavior and residual strength of post-fire concrete filled steel tubular columns. *Journal of Constructional Steel Research*, **112**, 282-292.

Yuan J. (2017) Reliability analysis of shear capacity of reinforced concrete beams. *Journal of Building Structures*, **38(4)**: 109-128.